DEVELOPMENT OF A 600MPA STRENGTH STEEL BY THERMOMECHANICAL PROCESSING OF A HIGH TITANIUM ALLOY IN A STECKEL PLATE MILL *

Cleiton Arlindo Martins [1]
Altair Lúcio de Souza [2]
Jorge Adam Cleto Cohn [3]
Geraldo Lúcio de Faria [4]
Marcello Arantes Rebellato [5]
Antônio Augusto Gorni [6]
Pello Uranga [7]
Jose Maria Rodríguez-Ibabe [8]

Abstract

The increasing need to obtain high levels of mechanical properties (yield strength – YS, and tensile strength – TS) has imposed several challenges on steel production processes. Load lifting machines are examples of applications that require YS > 600 MPa and TS > 680 MPa. In this scenario, HSLA steels has gained more relevance, given the possibility of increasing mechanical properties with carbon content decrease, favoring welding processes. Recent studies have shown the obtainment of YS above 600 MPa in alloys with 0.06% Nb and 0.1% titanium, in a ratio with nitrogen above the stoichiometric (Ti/N > 3.42). The addition of microalloying elements, associated with thermomechanical processing triggers the activation of hardening mechanisms such as grain refining and precipitation, however, it is necessary to adopt rolling strategies with strict control of process parameters. In this context, this work proposes the development of a hot-rolled steel strip aiming to reach YS > 600 MPa and TS > 680 MPa using a low carbon, Nb and Ti microalloyed alloy, with a Ti addition higher than the stoichiometric ratio and thermomecanically processed in a Steckel mill. Rolling parameters were determined considering microstructural evolution simulations performed in a software adjusted for the Steckel mill – the MicroSim-SM®. The non-recrystallization temperature was experimentally obtained by hot torsion test. Through dilatometry coupled to the strain cell, the alloy CCT diagram was obtained. Applying the above mentioned results, two different rolling strategies were proposed and evaluated in industrial scale. The rolled strips microstructure and mechanical properties were evaluated. It was possible to conclude that the applied methodology was efficient aiming to design a processing rout in order to reach a high level of grain refinement and a significant precipitation hardening that guaranteed the desired mechanical properties.

Keywords: Controlled Rolling, Thermomechanical Processing, Accelerated Cooling, High Strength Low Alloy Steels, Nb precipitation, Ti Stoichiometric, TiC precipitation

1 *MSc, Metallurgist Engineer, Rolling Mill Senor Specialist, Steckel Mill, Gerdau, Ouro Branco-MG, Brazil..*
2 *MSc, Metallurgist Engineer, R&D Senior Specialist, Gerdau, Ouro Branco-MG, Brazil.*
3 *MSc, Metallurgist Engineer, Technical Manager, Gerdau, Ouro Branco-MG, Brazil.*
4 *Doctor, Physicist. Associate Professor. Metallurgical and Materials Engineering Department (DEMET), EM, UFOP, Ouro Preto-MG, Brazil.*
5 *Metallurgist Engineer, Companhia Brasileira de Mineração e Metalurgia, São Paulo-SP, Brazil..*
6 *Dr. Eng, MSc Eng, Materials Engineer, Technical Consultant, CBMM, São Paulo-SP, Brazil.*
7 *PhD, Associate Director of Division, Materials and Manufacturing Division, CEIT and Universidad de Navarra, San Sebastian, Basque Country, Spain.*
8 *Dr Eng, Industrial Engineer; Senior Researcher, Centro de Estudios e Investigaciones Técnicas, Donostia-San Sebastián, Spain.*

** Technical contribution to the 57º Seminário de Laminação e Conformação de Metais, part of the ABM Week 6th edition, June 7th-9th, 2022, São Paulo, SP, Brazil.*

1 INTRODUCTION

Sectors such as machinery and equipment have increasingly demanded steels with high levels of mechanical properties. Load lifting structures are examples of applications that require a yield strength above 600 MPa and tensile strength above 680 MPa. In this scenario, HSLA steels gain relevance because they have the ability to reconcile high values of mechanical strength and toughness with low carbon contents, which make them suitable for applications where the use of welding processes is necessary. HSLA steels may contain micro additions of niobium (Nb) and titanium (Ti) that contribute to the final product having a ferritic-pearlitic microstructure with a high level of refinement, in addition to allowing considerable precipitation hardening. However, the microstructural refinement and activation of the precipitation hardening mechanism is conditioned to a strict control of the rolling process parameters. For this, production strategies must include thermomechanical processing in the rolling route. In the industrial scenario, controlled rolling followed by accelerated cooling is one of the most used processes. When associated with thermomechanical processing, the addition of 0.030% to 0.060% Nb has the ability to reduce the temperature range in which recrystallization occurs between rolling passes, resulting in a refined and homogeneous microstructure at the end of rolling [1]. The main contribution of Ti is in the formation of TiC precipitates at the end of rolling, during the cooling process. According to Elderman and Wigman [2], to obtain yield strength above 600 MPa in this alloy is directly associated with an effective titanium value above 0.06%, calculated through Equation 1. Recent studies show that another important prerequisite is the Ti/N ratio present in HSLA steels, which must be kept above the stoichiometric value – Ti/N > 3,42 [3].

$$\boldsymbol{Ti_{eff}}\% = \boldsymbol{Ti_{total}}\,\% - (\mathbf{3.4} \times \boldsymbol{N}\,\%) - (\mathbf{1.5} \times \boldsymbol{S}\,\%) \quad (1).$$

The production of HSLA steels in Steckel mills still has several knowledge gaps to be filled. The Steckel rolling mill is an equipment that has only one rolling stand positioned between two furnaces, provided with a rotating cylinder that has the objective of coiling the strip during the finishing rolling process, minimizing the heat loss due to the storage of the strip inside the furnaces [4]. In this context, this work aims to plan a thermomechanical rolling route for a HSLA steel microalloyed to Nb and Ti, with the addition of titanium above the stoichiometric ratio with nitrogen (Ti/N > 3.4), aiming to achieve a minimum yield strength of 600 MPa and a minimum tensile strength of 680 MPa in a Steckel mill. As support for the development, was used a software capable of modelling the microstructural evolution of austenite during rolling through equations based on the average size of the austenitic grains and on the parameters of the forming process (deformation per pass, deformation rate and temperature) – The MicroSim-SM® [5]. The non-recrystallization temperature of the alloy under study was experimentally obtained by hot torsion tests. Through the technique of dilatometry coupled to strain cells, it was possible to obtain the transformation curves under continuous cooling and determine the CCT diagram of the alloy in different rolling strategies, considering a previous recrystallized and pancaked austenite, allowing the evaluation of each morphology in the final microstructure. Based on the results obtained in the above mentioned characterization, two rolling routes were industrially planned and executed. The strips produced were microstructurally and mechanically characterized in order to evaluate the success of the development of the target product.

2 MATERIAL AND METHODS

2.1 Materials

The table 1 presents the chemical composition of the alloy under study, obtained by optical emission spectrometry on a sample taken from ingot slabs. The effective titanium value calculated based on Equation (1) was 0.07%, a result of the low sulphur and nitrogen contents presented, in addition to the high titanium content obtained. The Ti/N ratio presented a value of approximately 16, which is well above the stoichiometric value of 3.42.

Table 1. Chemical composition of the steel under study.

C	Mn	Nb	Ti	N
< 0,08	> 1,5	> 0,05	> 0,09	< 0,01

2.2 Experimental procedures

2.2.1 Physical simulations – determination of Tnr.

A The experimental determination of the non-recrystallization temperature (Tnr) was obtained through physical simulation in a hot torsion machine and followed the methodology proposed by Boratto *et al.* [7]. A deformation per pass of 0.2% and a time of 10 seconds between passes were used as parameters. The specimen was reheated for 15 minutes at a temperature of 1180°C and the strain rate used in each pass was $3s^{-1}$.

2.2.2 Physical simulations - determination of the alloy CCT diagram.

For the determination of the CCT diagram of the alloy, the application of 3 different thermal cycles was foreseen as shown in Figure 1. The objective of proposing these 3 different conditions was to evaluate, through dilatometric tests with deformation cell, the effect of the austenite previous condition on the curves of the CCT diagram. Thus, it was predicted a thermal cycle coming from a completely recrystallized austenite and two other cycles that started from pancaked austenite, with different degrees of accumulated deformation. With a reheat temperature of 1180°C, the cycles were predicted as follows:

- Cycle A: One strain pass at 1080°C (ε = 0,3%, $\dot{\varepsilon}$ = $1s^{-1}$) - recrystallized austenite.
- Cycle B: One strain pass at 1080°C (ε = 0,3%, $\dot{\varepsilon}$ = $1s^{-1}$), followed by one strain pass at 900°C (ε = 0,4%, $\dot{\varepsilon}$ = $1s^{-1}$) - pancaked austenite.
- Cycle C: One strain pass at 1080°C (ε = 0,3%, $\dot{\varepsilon}$ = $1s^{-1}$) followed by one strain pass at 900°C (ε = 0,4%, $\dot{\varepsilon}$ = $1s^{-1}$) and, finally, one more strain pass at 900°C (ε = 0,4%, $\dot{\varepsilon}$ = $1s^{-1}$) - pancaked austenite.

In the three cycles were applied cooling rates of 5, 10, 20, 25, 30, 35, 40, 60, 80 and 100 °C/s to determine the critical transformation temperatures. From the dilatometry tests, expansion curves were obtained, as well as the evolution of the transformed fraction as a function of temperature. Based on these results, the start and end temperatures of the transformations were determined for each applied cooling rate. In the CCT diagrams, the transformation start and end temperatures were determined as

5 and 95% of the transformed fractions, respectively. For the execution of this experimental step, a dilatometer model Bähr 805D was used.

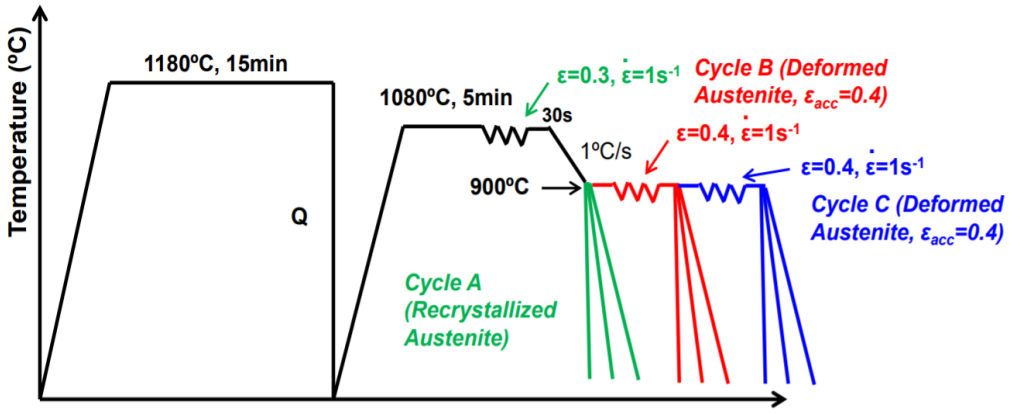

Figure 1. Thermal cycles performed to determine the CCT diagram.

2.2.3 Computer simulations via MicroSim-SM®

According to Uranga et al. (2016) [6], in MicroSim-SM®, the microstructural evolution of austenite during rolling is modeled by equations based on the average size of the austenitic grains and on the parameters of the rolling process (strain per pass, strain rate and temperature). Through interactions with the software, it is possible to optimize the rolling strategy to be adopted, aiming at a higher level of microstructural refinement and homogeneity. Different scales of rolling passes were evaluated, varying the percentages of reduction in each pass, both in the roughing and finish rolling. As a result of the simulations, for each rolling pass it was calculated: 1) recrystallized fraction (fraction of recrystallized austenitic grains); 2) The non-recrystallized fraction, 3) Average austenitic grain size (D mean); 4) Critical grain size (Dc 0.1); 5) Maximum austenitic grain size.

2.2.4 Rolling of strips and laboratory analysis

From the results obtained in the physical and computer simulations, two rolling strategies were planned with the objective of maximizing the microstructural refinement of the final product, and, consequently, activating the hardening mechanism by grain refining. The maximum volume of TiC precipitation was also aimed, which also resulted in a gain of mechanical properties through the precipitation hardening mechanism. The strips were rolled to a final thickness of 8.00 mm in the Steckel mill at the Gerdau Ouro Branco's unit. The strips were produced using thermomechanical processing (controlled rolling) and accelerated cooling after rolling. The coils were cooled at two different temperature levels, above and below 600°C. As the literature discusses, there is a narrow range of cooling temperature which can favor the precipitation of TiC during and/or after this stage, allowing an increase in properties. This temperature range was identified between 600°C and 650°C in continuous rolling mills [8]. The influence of coiling temperature on the mechanical properties was also investigated at this stage. Representative samples were taken from the strips and tensile tests were carried out in accordance with ABNT NBR 6673 [9]. An evaluation of the ferritic grain size distribution was also carried out via SEM – EBSD.

3 RESULTS AND DISCUSSION

3.1 Determination of Tnr

Figure 2 shows the graph of mean flow stress versus temperature obtained in a hot torsion test, using as parameters a deformation per pass of 0.2% and a time of 10 seconds between passes. The specimen was reheated for 15 minutes at 1180 °C, the same temperature adopted in the reheating of the specimens used in the determination of the CCT diagram. The strain rate used in each pass was 3 s^{-1}. It was possible to define the Tnr by identifying the point where the change in the slope of the curve occurs at 992°C, as proposed by Boratto *et al* [7]. In addition, critical temperatures Ar3 (beginning of austenite decomposition) at 770°C and Ar1 (end of austenite decomposition), which presented a value of 730°C, were also defined. These values are consistent with those indicated in the literature for steels with similar chemical composition [10,11].

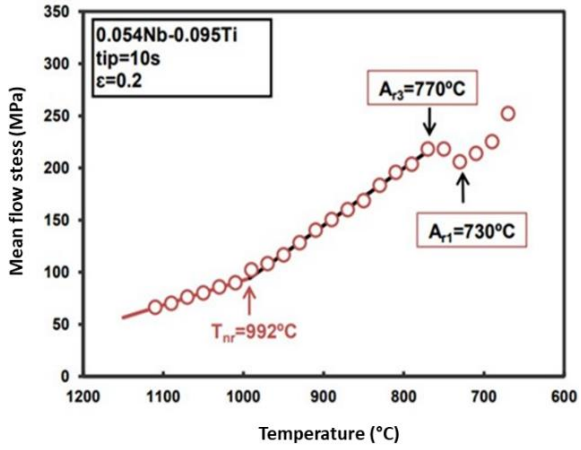

Figure 2. Mean flow stress curve versus temperature obtained through hot torsion tests for the steel under study - Tnr (992°C), Ar_3 (770 °C) e Ar_1 (730 °C).

3.2 Effect of austenite conditioning on alloy CCT diagrams.

According to the methodology for calculating the solubilization temperature predicted by Irvine [12], the complete curve for the volumetric fraction of solubilized niobium versus reheating temperature was plotted and is shown in Figure 3. Thus, the heating temperature for the specimens to be used in the determination of the CCT diagram was defined at 1180°C. The three CCT diagrams were plotted and are shown in Figure 4. In addition to regions of phase stability, cooling rates and Vickers hardness are also shown.

The first deformation step at 1080°C, for the three proposed cycles, was carried out with the objective of guaranteeing a more refined recrystallized austenitic structure. As verified in item 3.1, the Tnr of the alloy studied was 992°C. In this context, by applying a strain of 0.3% at a temperature of 1080°C (higher than Tnr), a complete recrystallization was promoted [13]. In Cycle B, a second deformation pass was applied at a temperature of 950°C, therefore, below the Tnr. The objective was to accumulate deformation in the austenite before the phase transformation. In the cycle C the austenite strain accumulation was intensified before the transformation by applying two strain passes below the Tnr.

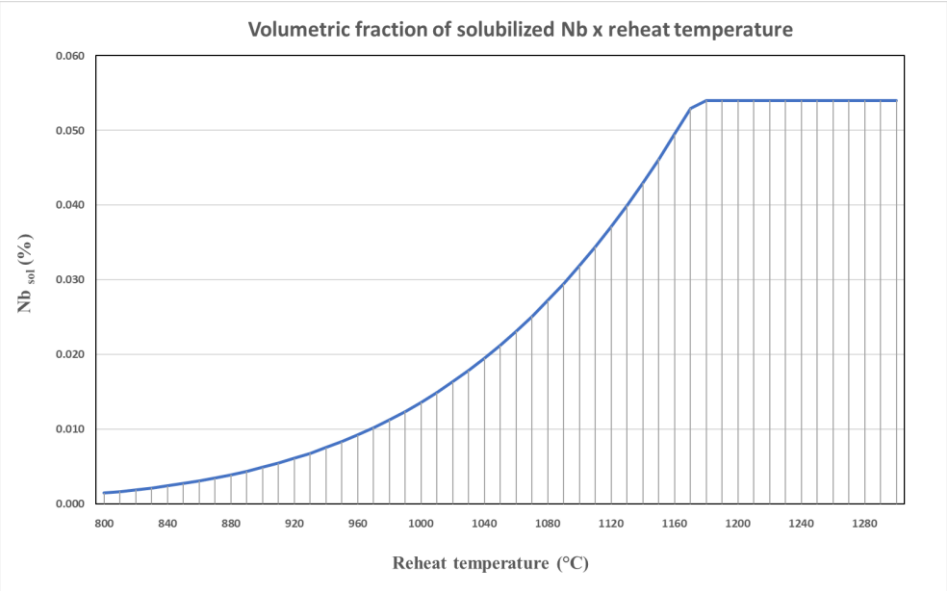

Figure 3: Reheating temperature x volumetric fraction of solubilized Nb for the steel under study, as predicted by Irvine [12].

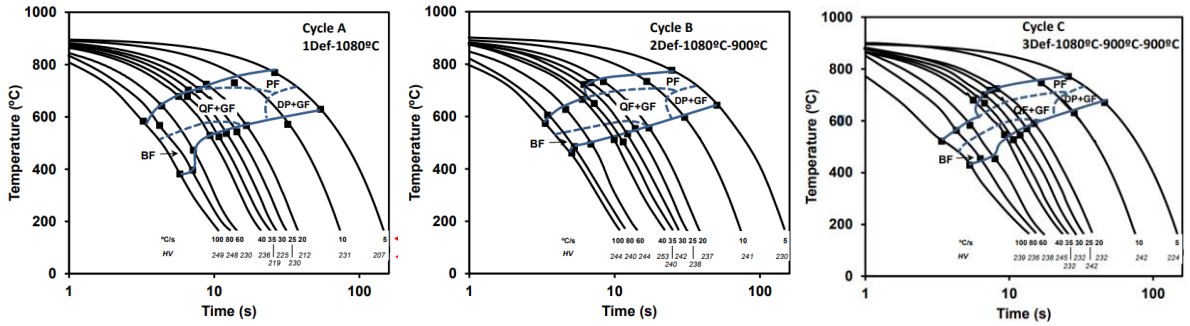

BF – bainitic ferrite / QF – quasi-polygonal ferrite / GF – granular ferrite / PF – polygonal ferrite / DP – degenerate pearlite

Figure 4. CCT diagrams obtained from the 3 proposed thermal cycles.

For cooling rates between 10 and 35ºC/s (usually used in industrial cooling systems), in cycle B, the transformation start temperatures are slightly higher, when transformation occurs from deformed austenite. The stability region of polygonal ferrite (PF) comprises a larger area of the diagram, extending to regions subjected to higher cooling rates. As an example, it is possible to verify that in cycle A, the formation of polygonal ferrite (PF) occurs only at rates lower than 25ºC/s, while for cycle B, ferritic grains with polygonal morphology are observed until cooling rates of 35ºC/s. This condition is explained by the fact that the accumulation of deformation in austenite (in Cycle B) promotes a slight increase in transformation temperatures, caused by the increase in the number of preferential active sites for ferrite nucleation, which is in agreement with what was reported by Ibabe (2014) [14]. Thus, for higher degrees of austenite deformation, it is possible for polygonal ferrite to form even at relatively high cooling rates. The possible occurrence, in greater quantity, of precipitation of Nb carbides from the deformed austenite could also contribute to the kinetics of polygonal ferrite formation, as there would be a decrease in the Nb and C contents in solid solution, which would justify a displacement of the CCT diagram to the left in relation to the diagram determined from a previous undeformed austenitic structure [15].

3.3 Computer simulations via MicroSim-SM®

The computer simulations using the MicroSim-SM® used as input parameters for the production of microalloyed steels already rolling in the Steckel mill at Gerdau Ouro Branco. Several rolling strategies were proposed and simulated by modifying MicroSim-SM® input parameters, such as percentage of reduction along rolling and reheat temperature. It was adopted a scale of passes with increasing percentages of reduction, as shown in Figure 5. Stalheim [11] shows that this is the best rolling strategy to be adopted when the objective is to maximize the microstructural refinement of austenite before the phase transformation. The percentage of reduction applied above the Tnr (roughing passes) was 80.5%. In this temperature region, the recrystallization process occurs at the end of each applied pass. The microstructural refinement in this phase comes from the solute drag mechanism. For the region below the experimentally defined Tnr, a total reduction of 73.2% was observed. Reductions applied at temperatures below Tnr result in a more refined final microstructure, as they come from austenitic pancake grains, that is, with a non-recrystallized structure [16]. There is also the formation of subgrains, which will later contribute to a greater final microstructural refinement. According to the simulation results obtained, the last three rolling passes (finishing passes) must be performed below the Tnr (best condition verified among those evaluated in the thermomechanical simulator).

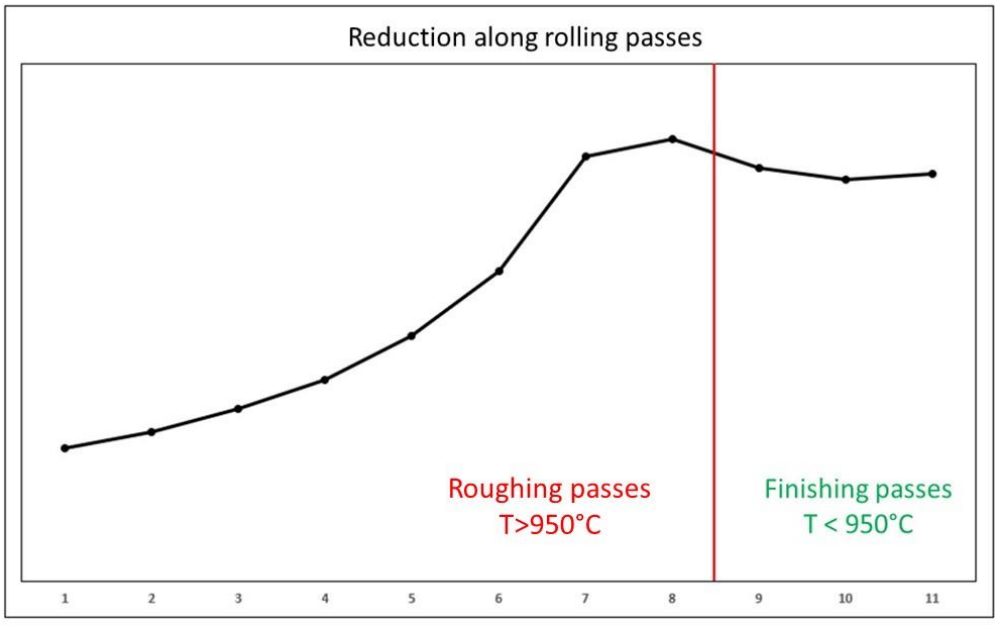

Figure 5. Reduction percentage during the rolling process.

The MicroSim-SM® simulated the evolution of the average austenitic grain size and the value of Dc01 along the rolling (Figure 6). The Dc01 parameter corresponds to the maximum austenitic grain size observed in each pass, considering 90% of the existing grains. This measure represents the heterogeneity of the microstructure, so that the closer the Dc01 value is to the mean value, the more homogeneous the microstructure.

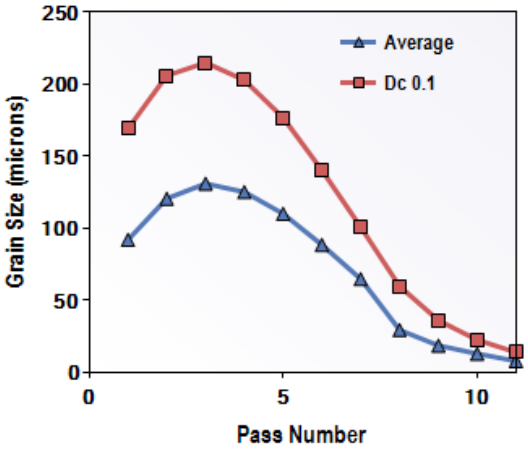

Figure 6. Simulations obtained via MicroSim-SM® for medium austenitic grain size and Dc01.

The simulation indicated an average austenitic grain size at the end of rolling of 8μm, with a Dc01 value of 14.1μm and a maximum austenitic grain size of 35μm, as shown in Figure 7. Blue bars represent recrystallized grains, while red bars represent non-recrystallized grains. The passes identified with the letter R (R1 to R8) are the roughing passes, while the passes starting with the letter F are the finishing passes. It is considered that there was no recrystallization if the percentage of non-recrystallized fraction is greater than 80%. It is possible to verify that in the three finishing passes (passes F9, F10 and F11) there was no recrystallization process, since they are performed below the Tnr. Rolling in the region of coexistence of recrystallized and non-recrystallized fraction was performed only in the eighth pass, presenting 85% of recrystallized fraction and 15% of non-recrystallized fraction. In the first seven passes there was 100% recrystallization. According to the literature [17], the intense deformation in the region of partial recrystallization can be harmful to the microstructural heterogeneity, which did not happen in the present study.

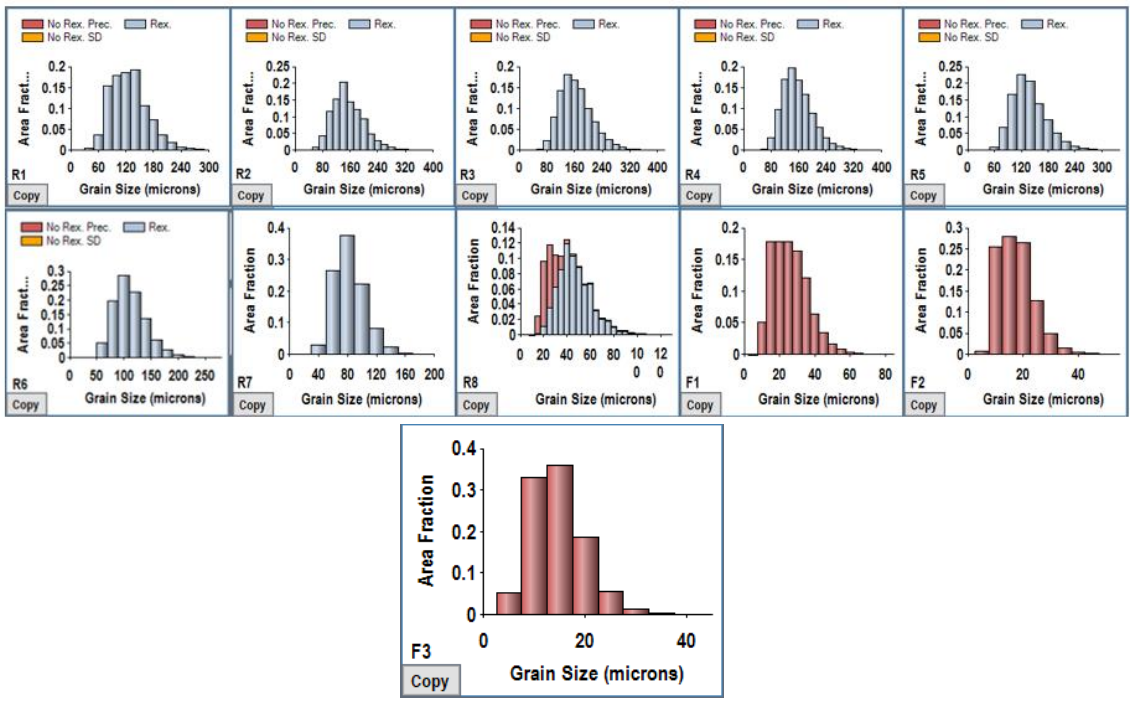

Figure 7. Evolution of austenitic grain size distribution per pass predicted by MicroSim-SM®.

3.4 Microstructural and mechanical characterization of rolled products

From the computer simulation via MicroSim-SM®, the rolling parameters were defined to obtain the highest level of microstructural refinement. The assumed Tnr was the one identified in the hot torsion test, which presented a value of 992°C. Figure 8 a) shows the ferritic grain size distribution obtained in one of the rolled strips, while Figure 8 b) shows a micrograph obtained through SEM-EBSD analysis of a particular region of the specimen. It is possible to verify that a high level of microstructural refinement was obtained. The boundaries located between 4º<ϑ<15º (in red) and ϑ>15º (in black) are considered as low and high angle boundaries, respectively. Low angle misorientation grains are assumed to contribute to strength properties due to their opposition to dislocation movement, whilst high angle boundaries are considered effective for controlling crack propagation [5]. The average grain size for the sample in Figure 8 b) was 2.4µm for low angle boundaries and 3.0µm for high angle boundaries.

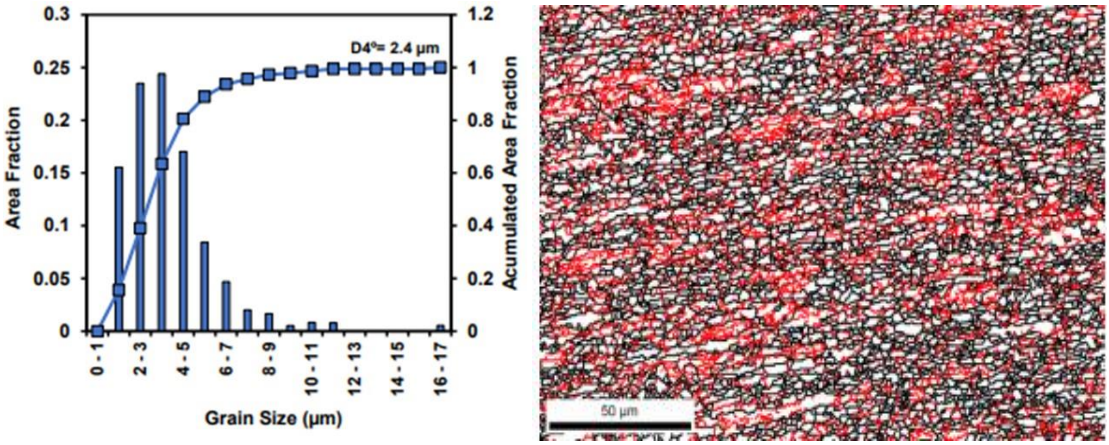

a) b)

Figure 8. a) Ferritic grain size distribution obtained in one of the rolled strips b) Image of the microstructure obtained via SEM-EBSD of the rolled strip.

The presence of Nb in thermomechanically processed HSLA steels guarantees the austenite conditioning throughout the hot deformation, producing a refined austenitic grain during rolling, which will result in an equally refined final grain. Nb has a strong influence on the recrystallization kinetics in hot rolling, acting as a retardant in the recovery and recrystallization of austenite, inhibiting grain growth if it is recrystallized. This effect is obtained by anchoring the dislocations in the grain boundaries and subgrains, leading to the “pancaking” of the microstructure (characterized by elongated grains) and the formation of deformation bands and subgrains. As a result, the formation of fine ferritic grains occurs after the phase transformation. Additionally, Nb also provides precipitation hardening. Similarly, 0.10% Ti in HSLA steels promotes the effect of inhibiting recrystallization [18]. The presence of fine particles of TiN and TiC helps to control the austenitic grain size during the rolling process, by delaying the recrystallization kinetics. In the cooling process, the precipitation of TiC helps to increase the strength of the rolled product.

In order to evaluate the effect of the coiling temperature on the final mechanical properties of the product, two rolling processes were carried out adopting different target coiling temperatures. In the first process, the increase in precipitation was prioritized as the green arrow indicates in the Figure 9. For this, the target coiling final temperature was above 600°C. Recent studies show that the coiling temperature that potentiates the largest volume of TiC precipitation is in the range of 600°C and 650°C [18,19]. The second cooling process was carried out in order to promote a greater volume of ferrite-bainitic structure in the final product, which will lead to an increase in yield strength and tensile strength by hardening governed by an increase in dislocation density. Thus, for the second process, the final coiling temperature below 600°C was targeted, as the blue arrow indicates in Figure 9.

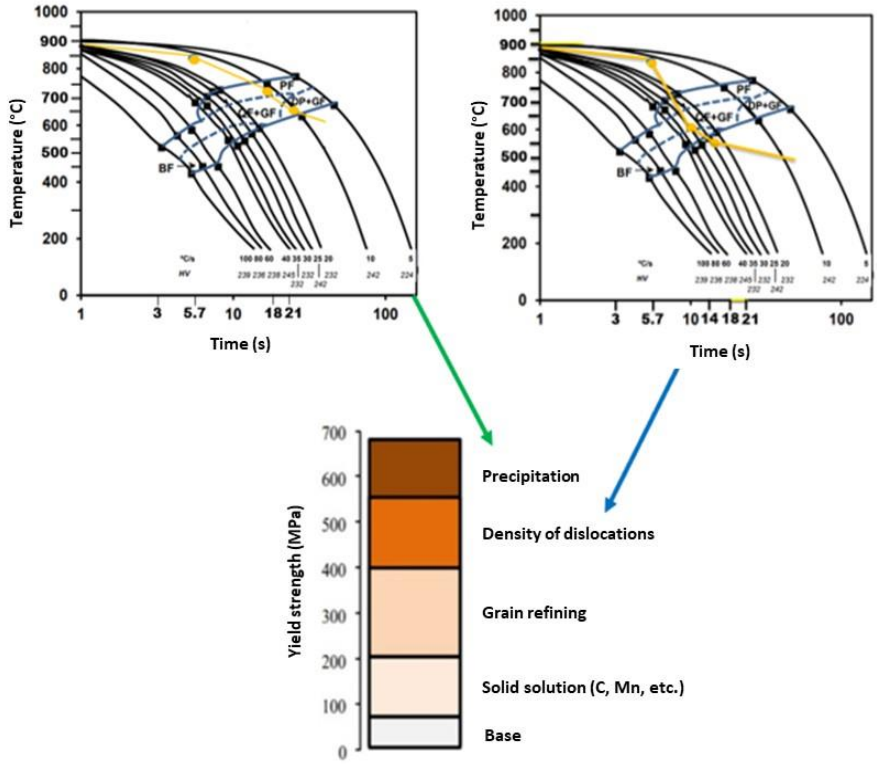

Figure 9. Strategies for rolling steel coils in studies.

Figures 10 and 11 show, respectively, the yield strength (YS) and the tensile strength (TS) as a function of the coiling temperature practiced on the strips. It is possible to verify that the highest values obtained are associated with coiling temperature above 600°C, with gains above 50 MPa in both YS and TS. Hardening due to grain refining and dislocation density contributed to the increase in YS and TS observed in the rolled strips in this study, however, in the case of coils produced at a coiling temperature equal or less than 600°C, the activation of the TiC precipitation process is inefficient, decreasing contribution of this mechanism in the formation of the YS and TS of the material. Results show that the occurrence of a precipitation hardening mechanism associated with the presence of TiC in HSLA steel with titanium content above the stoichiometric composition is essential to achieve minimum YS values of 600 MPa and TS values above 680 MPa in a Steckel mill.

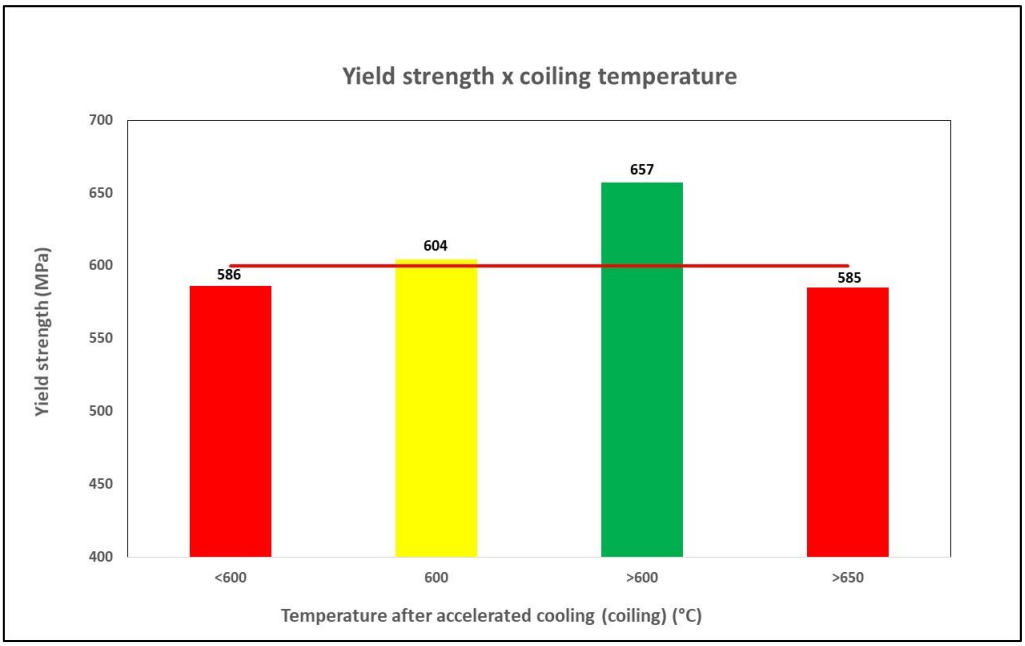

Figure 10. Yield strength x coiling temperature.

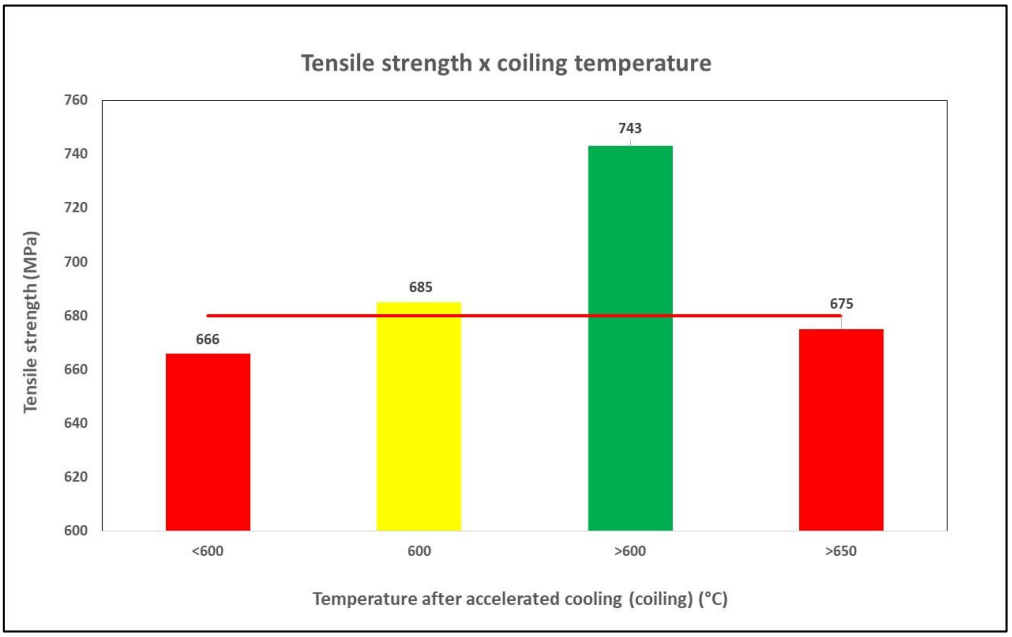

Figure 11. Tensile strength x coiling temperature.

4 CONCLUSION

The results show that the rolling product showed a high level of microstructural refinement, with average values of ferritic grain size in the range of 2.4μm to 3μm. YS above 650 MPa and TS above 700 MPa were obtained in a rolling strategy that prioritized the increase in precipitation hardening, with coiling temperature practiced above 600°C. These values indicate that the selection of the alloy with Ti above the stoichiometric, the process planning methodology used in this development, as well as the rolling strategy adopted were efficient to achieve the activation of the hardening

mechanisms by grain refining and precipitation hardening, promoted by the occurrence of TiC, necessary for the target product.

Acknowledgments

Gerdau Ouro Branco, Companhia Brasileira de Mineração e Metalurgia, CEIT/IK4 and Ouro Preto's federal university for all the support provided throughout the development of this work.

REFERENCES

1 BRUNA, R.; EBRI, G.; CERLIANI, A.; MORICONI, J.; GARCIA, C.I. A cost-effective approach to the development of high-strength-high-toughness NbVTi-based HSLA steels for the agricultural and heavy transportation industries. Iron & Steel Technology, 2018, pp. 66-72.
2 EDELMAN, D. G.; WIGMAN, S. L. method for producing titanium-bearing microalloyed high-strength low-alloy steel. U.S. Patent n.6,669,789. 2003.
3 BAKER, T.N. titanium microalloyed Steels. Ironmaking & Steelmaking, vol 46, no.1, pg 1-55, 2019.
4 RIZZO, E. M. S. Processos de laminação a quente de produtos planos de aço. Associação Brasileira de Metalurgia, Materiais e Mineração. São Paulo. 2011.
5 SOUZA, A.L.; OLIVEIRA, A. P. MARTINS, C.A.; BORGES, J.M.; LINO, J.J.P.; COHN, J. A. C.; TEIXEIRA, L.M.; ISASTI, N.; PEREDA, B.; URANGA, P. Microstructural Evolution during Steckel rolling and EBSD analyses of final microstructure. p. 599-608. In: 11th International Rolling Conference (IRC 2019), São Paulo, 2019.
6 URANGA, P.; IBABE, J.M.R.; STALHEIM, D.G.; BARBOSA, R.; REBELLATO, M. Application of practical modeling of microalloyed steels for improved metallurgy, productivity and cost reduction in hot strip mill applications. AISTech Proceedings, 2016.
7 BORATTO, F. J. M.; BARBOSA, R. A. N. M.; SANTOS, D. B.; Fundamentos da laminação controlada, Belo Horizonte, 1989.
8 SANTOS, A. A.; MURARI, F. D.; AVELAR JUNIOR, A. R.; PEREDA, B.; SORIA, B. L. Evolução microestrutural de aço da classe de 700 MPa na laminação de tiras a quente, p. 379-390. In: 55º Seminário de Laminação e Conformação, São Paulo, 2018.
9 Associação Brasileira de Normas Técnicas - NBR6673 - Produtos planos de aços - Determinação das propriedades mecânicas à tração - 1981.
10 SCHIAVO, C.P. Estudo da solubilização do Nb em aços microligados durante o reaquecimento de placas. Dissertação de mestrado apresentada ao Curso de Pós-Graduação em Engenharia Metalúrgica e de Minas da Universidade Federal de Minas Gerais, Belo Horizonte, 2010.
11 STALHEIM, D. G. Metallurgical and process strategy for the production of 700 MPa hot rolled structural steel coil, p. 745-756. In: 72nd ABM Annual Congress, São Paulo, 2017.
12 IRVINE, K.J.; PICKERING, F.B.; GLADMAN, T. Grain refined C-Mn Steels, journal of the iron and steel institute, v. 205, p. 161-182, 1967.
13 LINO, J.J.P.; COHN, J.A.C.; ROSSI, E.H; SOUZA, A.L.; FARIA, G.L.;SCHUWARTEN JÚNIOR, W. Laminação termomecânica de um aço microligado ao nióbio em um laminador de tiras a quente, com cadeira Steckel. p. 82-91. In: 53nd Rolling Seminar, Rio de Janeiro, 2016.
14 IBABE, J.M.R.; Metallurgical aspects of flat rolling process. The Making, Shaping and Treating of Steel, Flat Products Volume, AIST, 2014, pp. 113-170 (Chapter 3).
15 JIA, T.; MILITZER, M. The Effect of Solute Nb on the Austenite-to-Ferrite Transformation Metallurgical and materials transactions. A, Physical metallurgy and materials science, 2014-11-19, Vol.46 (2), p.614-621
16 HULKA, K. Fundamentals of the controlled rolling process, 2018.
17 ROCCISANO, A.; NAFISI, S. STALHEIM, D.; GHOMASHCHI, R. Effect of TMCP rolling schedules on the microstructure and performance of X70 steel. Materials Characterization, 178, 2021.
18 LARZABAL, G.; ISASTI, N.; RODRIGUEZ-IBABE, J. M.; URANGA, P. Evaluating strengthening and impact toughness mechanisms for ferritic and bainitic microstructures in Nb, Nb-Mo and Ti-Mo microalloyed steels. Metals, v. 7. 2017
19 PEREDA, B; GARCIA-SESMA, L.; LÓPEZ, B. Effect of coiling temperature on the hardening mechanisms of a high-Ti steel. Materials Science Forum, Vol. 941, pp 164-169, 2018.